Synthesizing Personalized Construction Safety Training Scenarios for VR Training

Wanwan Li, Haikun Huang, Tomay Solomon, Behzad Esmaeili, and Lap-Fai Yu

George Mason University

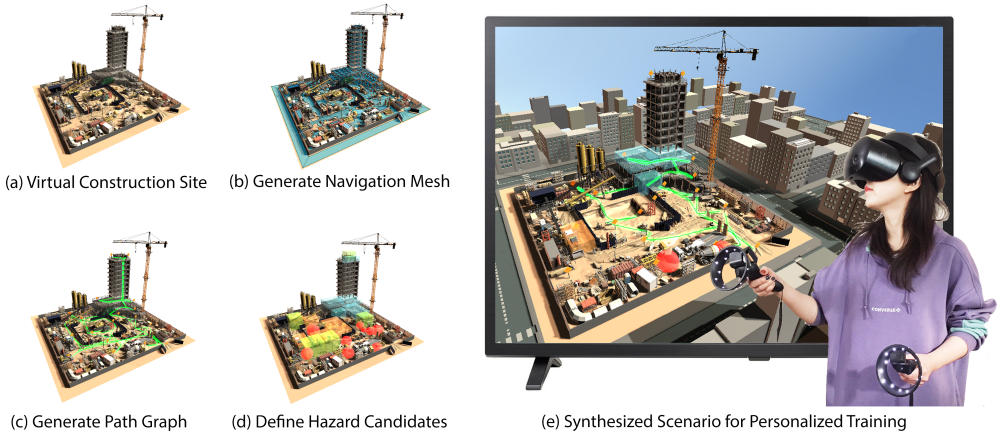

Fig. 1. Given a virtual construction site as input (a), after pre-processing steps (b-d), our optimization-based approach synthesizes personalized training scenarios by adding common construction hazards and generating training routes. (e) Users are guided through a generated route (green) and trained to inspect hazards in virtual reality.

Abstract—Construction industry has the largest number of preventable fatal injuries, providing effective safety training practices can play a significant role in reducing the number of fatalities. Building on recent advancements in virtual reality-based training, we devised a novel approach to synthesize construction safety training scenarios to train users on how to proficiently inspect the potential hazards on construction sites in virtual reality. Given the training specifications such as individual training preferences and target training time, we synthesize personalized VR training scenarios through an optimization approach. We validated our approach by conducting user studies where users went through our personalized guidance VR training, free exploration VR training, or slides training. Results suggest that personalized guidance VR training approach can more effectively improve users' construction hazard inspection skills.

Index Terms—virtual reality, construction safty, training, optimization, personalization

1 Introduction

In the construction industry, labor costs constitute 30-50% of total project costs [34]. Since construction companies typically only have a 2-3% profit margin, managing labor costs to enhance productivity while ensuring safety is critical [18]. In the current industry, lack of skilled labor is the main reason for cost overruns [44], loss of productivity [23], frequent safety incidents [2], schedule overruns [10], and decline in quality performance [22]. To improve their skills, construction workers must be trained; however, the traditional one-size-fits-all training approach has failed to fully prepare workers for current worksite challenges [19]. Therefore, developing personalized training programs for construction workers will have significant impacts in construction industry. It becomes pertinent to find efficient and effective safety training programs to amplify construction industry's labor supply.

Given the emerging technologies in the virtual reality industry, VR provides a practical platform to train people in a safe and efficient manner through serious virtual training tasks. Several research studies indicated that virtual reality, to some extent, can be a substitute for real-world task training [25, 29, 32, 33, 39]. Therefore, it is possible to leverage virtual reality to conduct construction safety training which is not easy to be achieved in reality [42]. Besides, compared to real-world training tasks, highly immersive virtual reality training can be more engaging through users' interactions or involvements [4, 48], injury-free [6, 13, 15] but stressful enough through alerts [12, 20, 36], enabling trainees to step forward easily and improve their skills efficiently.

Our work is inspired by prior works which use immersive virtual scenarios for simulating work processes on construction sites [1, 14, 35, 37, 40]. In contrast to the prior works which employ manually-designed construction scenarios, we devise an optimization-based approach to automatically synthesize personalized safety training scenarios to improve the users' skills in inspecting hazards on construction sites in virtual reality. As shown in Figure 1, given the training specifications such as an individual's training preferences and target training time, our approach automatically synthesize corresponding training scenarios through the simulated annealing method [43]. To validate the efficacy of our approach, we developed several virtual construction sites and conducted a series of user studies to analyze the users' performances before and after the VR training. Our major contributions include:

- Creating virtual construction sites with different types of common hazards and implementing a user-friendly interactive interface for construction safety training in virtual reality.

Manuscript received xx xxx. 201x; accepted xx xxx. 201x. Date of Publication xx xxx. 201x; date of current version xx xxx. 201x. For information on obtaining reprints of this article, please send e-mail to: reprints@ieee.org. Digital Object Identifier: xx.xxxx/TVCG.201x.xxxxxxx

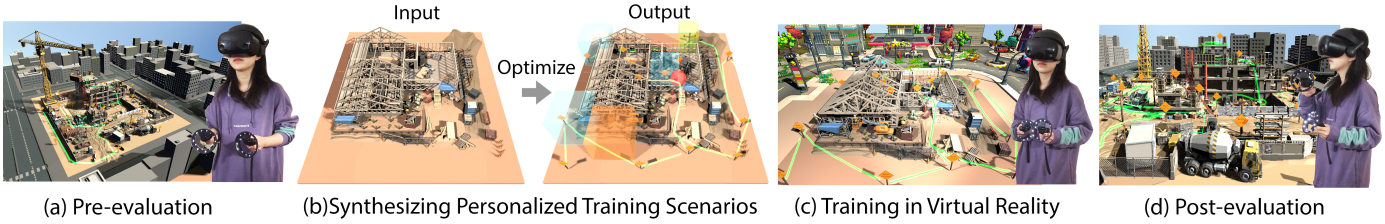

Fig. 2. Overview. (a) We pre-evaluate users' skills in identifying hazards on construction sites. (b) According to their performances in pre-evaluations, we synthesize personalized training scenarios to improve the users' weaknesses. (c) Users are trained through those synthesized training scenarios. (d) We post-evaluate the users' performance through the same tasks in pre-evaluation to measure their improvement.

- Devising an optimization-based approach to synthesize personalized training scenarios, which comprise navigation paths and hazard inspection tasks, for achieving specific training targets.
- Validating the effectiveness of our personalized guidance VR training scenarios through user studies and statistical analysis.

2 Related Work

Virtual Construction Safety Training. Conventional construction safety training approaches share a common drawback of the lack of trainees' engagement [7]. More innovative approaches and benchmarks [5, 28] are presented to improve construction safety training. To enable trainees to have control over their progress and achieve personal instructions in a safe environment, more attention is given to immersive virtual construction safety training [16, 26, 27]. In recent years, as virtual reality technologies become widespread, Sacks et al. [40] indicated that virtual construction safety training is feasible and effective, especially in terms of workers' learning, identifying, and inspecting construction safety risks. Aati et al. [1] developed an immersive virtual platform for enhancing the training for work zone inspectors, which is capable of replicating the experience of an inspector driving through a work zone in a safer, cheaper, and quicker way. Through the simulation of VR-based safety training programs developed by Zhao et al. [50], users can effectively promote their abilities for hazard inspection. On the other hand, augmented reality and augmented panoramas of reality technologies are applied to virtual construction safety training [16] and assembly training [45] to achieve immersive training experiences.

Furthermore, Eiris et al. [14] developed and compared two immersive virtual training platforms for hazard inspection, among which one is based on virtual reality while another is based on a 360-degree panoramic setup. Those works plot a trend that immersive virtual construction safety training is gaining popularity.

Personalized Virtual Training Synthesis. Most of the existing construction safety VR training programs work through repeatedly rehearsing similar tasks pre-programmed in the VR applications [50], which may lead to concerns on training effectiveness as real-world hazards occur randomly. Therefore, randomness was a consideration in the system proposed by Xie et al. [47] for creating many variations of the training scenarios. However, randomized hazard simulations make it non-trivial and technically challenging for the designers to create personalized training scenarios for VR training. As inspired by the recent works which successfully synthesized personalized training scenarios to help users improve certain skills such as driving skills [25] and wheelchair control [29], optimization techniques are applied to substitute manual configurations in creating effective training programs. Emerging optimization-based approaches such as optimization for exertion games [30, 46, 49], optimization for wayfinding design proposed by Huang et al. [21], and optimization for personalized functional workspace scene layout synthesis proposed by Liang et al. [31] show that stochastic optimization-based approaches are efficacious for synthesizing realistic virtual scenarios. Motivated by these works, we devise an optimization-based approach to synthesize personalized construction safety training scenarios for VR training.

3 Overview

As shown in Figure 2, we show the construction sites on our VR platform and synthesize the training scenarios where the users are pre-evaluated. A training scenario includes a route for users to navigate through (green curve) and a sequence of nearby hazards (colored regions) that need to be correctly identified by the users. Through optimizing the navigation route along with the sequence of nearby hazards in a fully automatic manner, our approach synthesizes the personalized training scenarios to improve the user's skills which are identified as weaknesses in the pre-evaluation. For example, a synthesized training will contain more fall hazards in case the user is not able to identify fall hazards in the pre-evaluation. In the end, we validate the effectiveness of our synthesized training scenarios by comparing the users' performances in the post-evaluation with the their performances in the pre-evaluation and testing the improvement in users' performances statistically. We validate that our approach can effectively improve the trainee's skills in inspecting construction safety hazards.

4 Training Scenario Synthesis

Hazard Types. According to the Center for Construction Research and Training [41], major construction hazards types include (a) Struck-by Hazards, (b) Fall Hazards, (c) Caught-In/between Hazards, and (d) Electrical Hazards as depicted in Figure 3.

In our optimization approach, we regard the struck-by hazards as dynamic hazards and other types of hazards as static hazards or potential hazards. Noted that this classification only applies to general situations. More strictly, in some special situations, struck-by hazards are not the only dynamic hazard. For example, sometimes caught-in/between hazards are dynamic as well when they are related to moving mechanical parts, or electrocution when the contact of a boom vehicle with a power line can also have a dynamic nature. However, in our approach, in order to separate the "moving and obvious" hazards that users need to avoid from those "hidden or potential" hazards that users to identify, we tag those moving hazards as "dynamic" and those staying hazards as "static". Our approach is scalable to consider more complex training scenarios with both dynamic and static features. The following elaborates the four types of common hazards for construction safety inspection training:

- Struck-by Hazards. As dynamic hazards, struck-by hazards are simulated through mechanical animations. During the VR training, struck-by hazards can directly run into the users when they are passing nearby.
- Fall Hazards. Refer to the hazards that could result in accidental falls. Examples include untied workers, no guardrail protection on hight, ladder hazards, and tripping hazards.
- Caught-In/between Hazards. Refer to the hazards that could crush people by objects from a side, such as cave-in hazards.
- Electrical Hazards. Refer to the hazards caused by electrical components, such as overhead power lines and no clearance between the power line and scaffold.

4.1 Cost Functions

In our approach, a training scenario is synthesized as a route and several hazards along the route. A route starts at the entrance of a construction site and ends at a random position. Route R along with H which is a list of hazards that users will experience sequentially are optimized with respect to the total cost function $C_{\text{total}}(R,H)$:

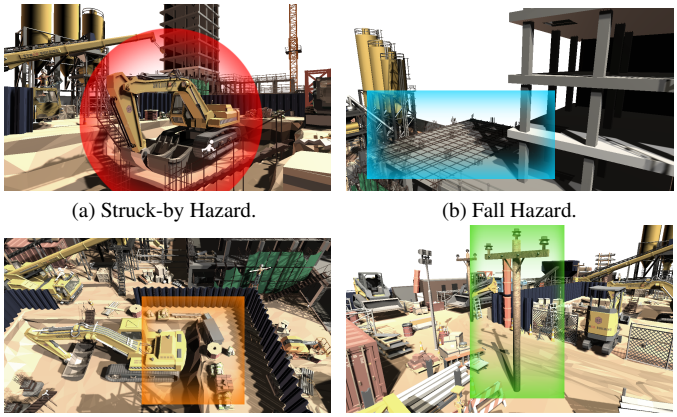

(a) Struck-by Hazard. (b) Fall Hazard.

(c) Caught-in/between Hazard. (d) Electrical Hazard.

Fig. 3. Examples of common hazards. (a) A struck-by hazard caused by the swing of excavator. (b) A fall hazard caused by missing guardrail protections. (c) A caught-in/between hazard caused by objects which are too close to a cave's edge. (d) An electrical hazard caused by an electrical component such as a light pole.

$$C_{\text{total}}(R,H) = w_{\text{D}}C_{\text{D}}(R,H) + w_{\text{S}}C_{\text{S}}(R,H) + w_{\text{T}}C_{\text{T}}(R,H), \quad (1)$$

where the dynamic hazard cost $C_{\text{D}}(R,H)$ encodes how likely the user will encounter dynamic hazards such as struck-by hazards H when navigating along the route R; the static hazard cost $C_{\text{S}}(R,H)$ encodes the user's preferred training targets with respect to the user's proficiency in identifying different types of static hazards such as fall, caught-in/between and electrical hazards; and the training time cost $C_{\text{T}}(R,H)$ encodes the target amount of training time. w_{D}, w_{S}, and w_{T} represent the respective blending weights of the cost terms.

Dynamic Hazard Cost. During training process, dynamic hazards such as struck-by hazards are simulated through mechanical animations to mimic the vital accidents that are likely to happen during the construction process in the real world. The spatial distribution of dynamic hazards affects the difficulty of safety inspection training. For example, if the dynamic hazards are present near the navigating route, it is more challenging for the user to identify other nearby static hazards while avoiding being struck by the dynamic hazards. On the other hand, if the route is passing through spaces without dynamic hazards, it is much easier for the user to focus on inspecting the static hazards, in this case, the training is less challenging. Let $D(R,H)$ be a function proportional to the conditional probability of the occurrence of any dynamic hazard H that may happen along a route R, we evaluate the dynamic hazard cost function $C_{\text{D}}(R,H)$ by measuring the difference between that estimated probability $D(R,H)$ and user's target occurrence probability of dynamic hazards λ_{D} as:

$$C_{\text{D}}(R,H) = 1 - \exp(-\left(\frac{D(R,H) - \lambda_{\text{D}}}{\sigma_{\text{D}}}\right)^2), \quad (2)$$

where we empirically set $\sigma_{\text{D}} = 0.25$.

Hazard Probability. Dynamic hazards involve moving objects on the virtual construction site, we introduce the conditional probability to evaluate the probability of the occurrence of hazardous accidents. Given any point $\mathbf{r}$ on route R, let $d(\mathbf{r},H_i)$ denote the distance between $\mathbf{r}$ and the center of a hazard H_i. Let $\delta(H_i)$ denote the affecting range of hazard H_i. Then, given the condition that if point $\mathbf{r}$ is close enough to the hazard H_i, namely, $d(\mathbf{r},H_i) < \delta(H_i)$, we define the conditional probability of the occurrence for each hazard H_i as $\Pr(H_i|d(\mathbf{r},H_i) < \delta(H_i))$. So, we evaluate the overall probability $D(R,H)$ that any dynamic hazardous events may happen along route R as a function proportional to the summation of line integral for the conditional probability of each hazard H_i along route R:

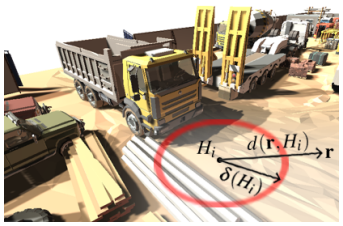

Fig. 4. Dynamic hazard notations.

$$D(R,H) = \frac{k}{|R|}\sum_{i=1}^{|H|}\int_R \Pr(H_i|d(\mathbf{r},H_i) < \delta(H_i))\mathrm{d}\mathbf{r}, \quad (3)$$

where the number $|H|$ is the total amount of synthesized hazards H; the $|R|$ is the total length of the route calculated through the line integral along the route R; and k is a fine-tuned scale factor to adjust the overall dynamic hazardous probability returning the values evenly distributed within $[0,1]$. Empirically, we set $k = 0.3$.

We simulate the dynamic hazards through periodic motions of a vehicle, a truck, or an excavator. Let $T_{d(B_i,H_i)<\delta(H_i)}$ denote the period time that dynamic hazard H_i's corresponding moving object (e.g., a vehicle.)'s bounding box B_i enters H_i's affecting range $\delta(H_i)$. Let $T_{d(B_i,H_i)\geq\delta(H_i)}$ denote the period time that H_i's moving object's bounding box B_i is outside the affecting range. Then, the dynamic hazard H_i's conditional probability $\Pr(H_i|d(\mathbf{r},H_i) < \delta(H_i))$ is:

$$\Pr(H_i|d(\mathbf{r},H_i) < \delta(H_i)) = \frac{T_{d(B_i,H_i)<\delta(H_i)}}{T_{d(B_i,H_i)<\delta(H_i)} + T_{d(B_i,H_i)\geq\delta(H_i)}}, \quad (4)$$

where $\mathbf{r}$ is the position of an arbitrary point on route R'.

Static Hazard Cost. Given user's performance in the pre-evaluation, we synthesize personalized training scenarios to improve the specific skills that the user shows weaknesses. In other words, we want to improve the user's skills of inspecting certain types of static hazards. More specifically, given M different types of static hazards, let the target occurrence probability for the jth type of hazard be λ_j, where $j = 1,2,...,M$. A large λ_j means that static hazards of the jth type appear more frequently in the training scenario. We encode such target occurrence probabilities through the static hazard cost function $C_{\text{S}}(R,H)$:

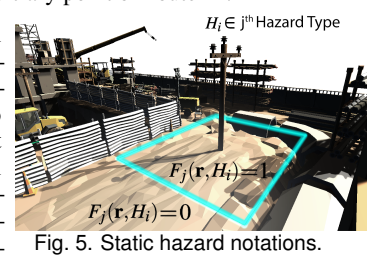

Fig. 5. Static hazard notations.

$$C_{\text{S}}(R,H) = 1 - \exp(-\left(\frac{S(R,H)}{\sigma_{\text{S}}}\right)^2), \quad (5)$$

where we empirically set $\sigma_{\text{S}} = 0.25$. $S(R,H)$ measures the difference between the probabilities of different types of hazards appearing near the route R and the target occurrence probabilities:

$$S(R,H) = \frac{1}{M}\sum_{j=1}^{M}\left(\frac{k}{|R|}\sum_{i=1}^{|H|}\int_R F_j(\mathbf{r},H_i)\mathrm{d}\mathbf{r} - \lambda_j\right)^2, \quad (6)$$

where the hazard score function $F_j(\mathbf{r},H_i)$ returns 1 when the hazard H_i appears within the route point $\mathbf{r}$'s nearby region and H_i belongs to the jth type of static hazard; Otherwise, it returns 0. $|H|$ denotes the total amount of synthesized hazards H. $|R|$ is the total length of the route R. k is a scaling factor for adjusting each term value to be evenly distributed between 0 and 1. Empirically, we set $k = 0.2$.

Training Time Cost. The training time cost function $C_{\text{T}}(R,H)$ measures the difference between the estimated training time $T(R,H)$ navigating through the route R and the target training time ρ_{T}:

$$C_{\text{T}}(R,H) = 1 - \exp(-\left(\frac{T(R,H) - \rho_{\text{T}}}{\sigma_{\text{T}}}\right)^2), \quad (7)$$

where we empirically set $\sigma_{\text{T}} = 2\rho_{\text{T}}$. The total training time $T(R,H)$ includes the amount of time for navigating along the route R and the amount of time for inspecting all hazards:

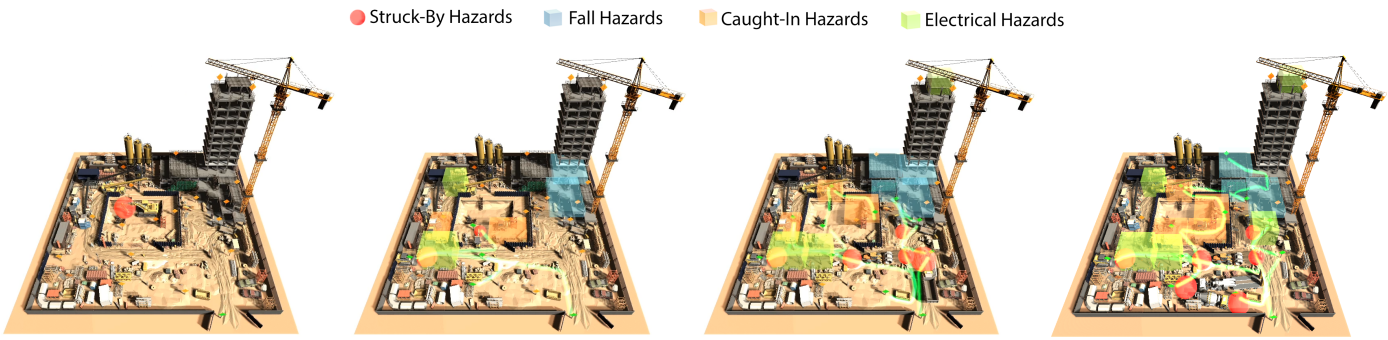

(a) The 1st iteration. (b) The 100th iteration. (c) The 200th iteration. (d) The 500th iteration (Result).

Fig. 6. An example of the optimization process. Green curves are the synthesized navigation routes. (a) The route is initialized at the entrance of the construction site. Throughout the iterations, vertices are randomly added to, replaced by, or removed from the current navigation routes. Different types of hazards (colored in red, blue, yellow, or green) are randomly added, replaced, or removed. Figure (b-d) shows the intermediate results generated through the optimization process. Figure (d) shows the result of the final synthesized training scenario.

$$T(R,H) = k_1 \frac{1}{v} \int_R \mathrm{d}\mathbf{r} + k_2 \sum_{i=1}^{|H|} t(H_i), \tag{8}$$

where $|H|$ is the total number of synthesized hazards H. Pre-defined constant v is the users' default navigation speed. The line integral along the route returns the total length of the route, which is divided by the constant velocity to give the time for traversing the route R. $t(H_i)$ is the estimated time to finish inspecting hazard H_i. By setting up a timer in the program, we count the average time taken by the users for identifying each type of hazard according to the statistical analysis of a pilot study. For more details, please refer to the supplementary material. k_1 and k_2 are two balancing factors used to balance the importance of the two considerations: path navigation time and hazard inspection time. During the training, users are prompt to specify the hazards while navigating. As navigation time plays a more important role in estimating the overall training time, we empirically set a larger $k_1 = 0.8$ and a smaller $k_2 = 0.2$.

4.2 Optimization

Given the training specifications such as the total training time and the target occurrence probabilities of different types of hazards, our approach synthesizes a navigation route R and the hazards list H by optimizing with respect to the total cost function.

To synthesize realistic navigation routes, we generate a navigation mesh on the input virtual construction site. We randomly pick some points of interest within the scene and put signs (work ahead signs indicating hazards) at those random points. In this way, the training routes can be assembled through those shortest navigation paths between every two signs. Such configurations form a navigation graph structure where the signs are the vertices and the navigation paths connecting two signs are the edges connecting two vertices. Empirically, we formalize the navigation graph as a k-regular graph [38] with k-shortest distance navigation paths connecting every two vertices [8], where we set $k = 4$. Hereby, a synthesized route R consists of an arbitrary number of vertices and the edges connecting every two adjacent vertices.

Fig. 7. A work sign.

As shown in Figure 6, the initialization of the route R contains only one vertex, which represents both the starting point and ending point, and does not constitute any edge. This starting point corresponds to the location of the construction site's entrance. We formulate the optimization problem as a graph searching problem by employing the Markov chain Monte Carlo method [17] to search for a solution that minimizes the total cost function. Given any randomly chosen vertex v on the current route R, a new route R' is randomly proposed within the solution space through one type of moves described as follows:

- *Add a Vertex*: a random vertex v' adjacent to v is added to the current route R to create a proposed route R'.
- *Remove a Vertex*: the vertex v is removed from the current route R to create a proposed route R' while keeping the connectivity.
- *Modify a Vertex*: the vertex v is replaced by a random vertex v' adjacent to v to create a proposed route R'.

Similarly, given the current list of hazards H, a new list of hazards H' is proposed by randomly searching within the solution space through three types of moves:

- *Add a Hazard*: a random hazard is added to the current list of hazards H to create a proposed list of hazards H'.
- *Remove a Hazard*: a random hazard is removed from current list of hazards H to create a proposed list of hazards H'.
- *Modify a Hazard*: a random hazard in the current list of hazards H is replaced by another random hazard not in the current list to create a proposed list of hazards H'.

After generating the proposed route R' and proposed hazards H', our approach uses the Metropolis criterion of the simulated annealing technique [11, 24] to determine the acceptance probability $\Pr(R', H'|R, H)$ for accepting the proposed route and hazards:

$$\Pr(R', H'|R, H) = \min(1, \frac{f(R', H')}{f(R, H)}), \tag{9}$$

where $f(R, H)$ is a Boltzmann-like objective function encoding the total cost function:

$$f(R, H) = \exp(-\frac{1}{t} C_{\text{total}}(R, H)), \tag{10}$$

where t is the temperature parameter of simulated annealing, which decreases gradually throughout the optimization. As the temperature t decreases over iterations, the optimizer becomes less aggressive and more greedy. By the end, as the temperature drops to a low value near zero, the optimizer tends to accept better solutions only. We empirically use temperature $t = 1.0$ at the beginning of the optimization and decrease it by 0.2 every 100 iterations until it reaches zero. The optimization process is terminated if the total cost change is smaller than 3% over the past 50 iterations.

Parameter Settings. Unless otherwise specified, we set the training time cost's weight $w_{\text{T}} = 0.2$, dynamic hazard cost's weight $w_{\text{D}} = 0.4$, and the static hazard cost's weight $w_{\text{S}} = 0.4$. We set an overall training time $\rho_{\text{T}} = 10$ minutes as a soft regularization term to avoid overly short or long training. The setting will result in a synthesized training scenario comprising a route with a total length of about 400m to 500m (2 to 4 minutes walking distance) and 6 to 12 selected hazards nearby the route. During the training, the user may use the controller's speed-up button to increase the navigation speed so that to shorten the training

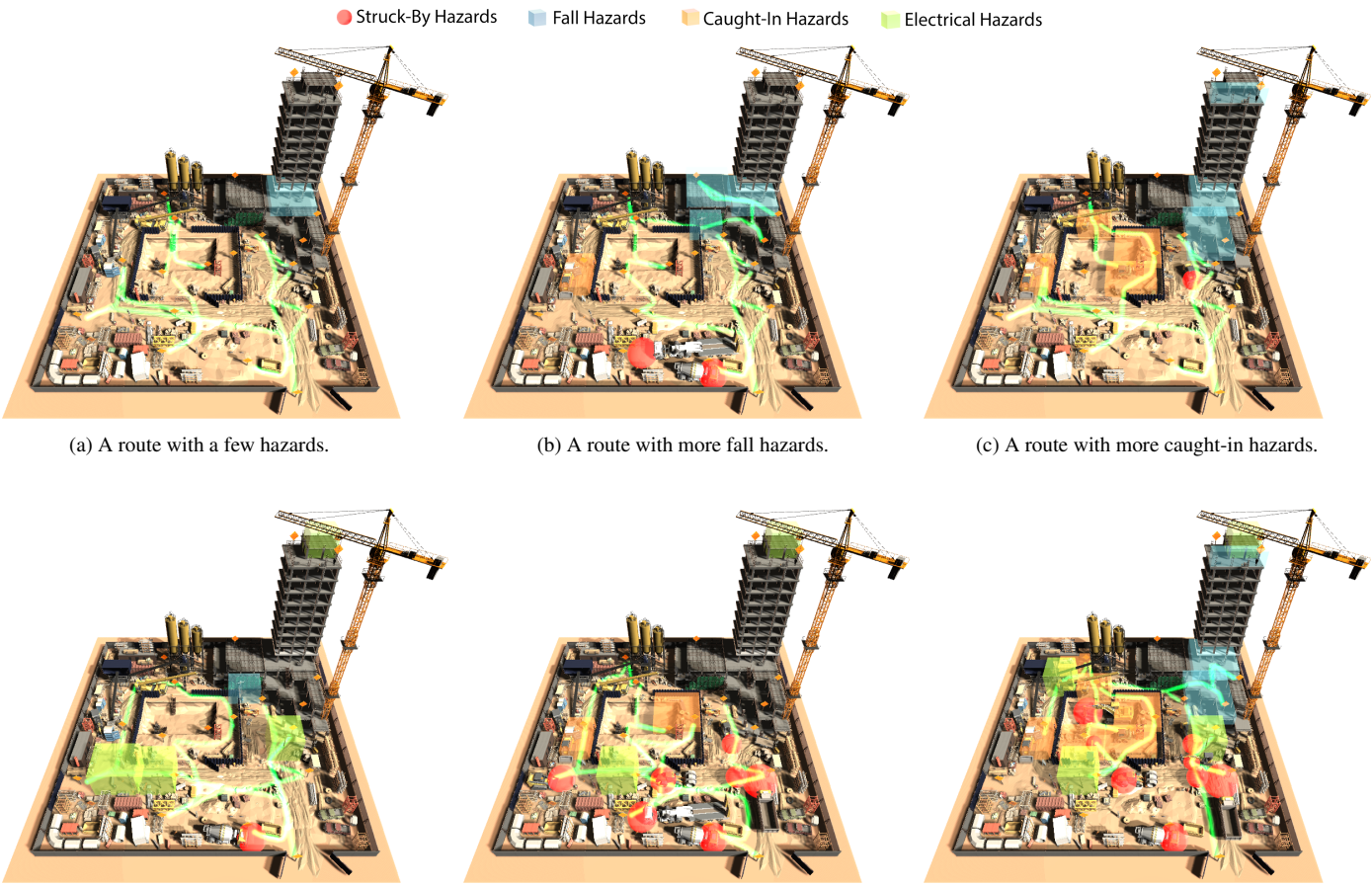

(a) A route with a few hazards.

(b) A route with more fall hazards.

(c) A route with more caught-in hazards.

(d) A route with more electrical hazards.

(e) A route with more struck-by hazards.

(f) A route with all types of hazards.

Fig. 8. Synthesized training scenarios on the same construction site. Green curves are the navigation routes. Six different scenarios are shown, including (a) a route passing through a few hazardous regions; (b) a route passing through more regions with fall hazards (blue); (c) a route passing through more regions with caught-in/between hazards (yellow); (d) a route passing through more regions with electrical hazards (green); (e) a route passing through more regions with struck-by hazards (red); and (f) a route passing through regions with all types of hazards.

time. Figure 8 shows some training scenarios synthesized with these parameter settings on a construction site. Please refer supplementary material for synthesized training scenarios on another construction site.

Personalized Training Targets. As shown in Figure 8, different target occurrence probabilities of different types of hazards are applied for generating different training scenarios on a construction site. As discussed in Section 4.1, adjusting the target occurrence probability λ_j for each type of hazard will synthesize training scenarios with different emphases on the types of hazards present. Intuitively, if a user is weak in identifying a certain type of hazard in the pre-evaluation, we then synthesize virtual training scenarios containing more of that type of hazards to reinforce the user's inspection skill correspondingly.

To demonstrate the capability of our optimization-based approach for synthesizing different training scenarios focusing on different hazard types, we manually specify six different personalized preference parameter settings for synthesizing the results shown in Figure 8. Note that, in practice, such personalized parameters can instead be estimated from a user's performance in the pre-evaluation.

We specify a low occurrence probability of a type of hazards as 0.1 and a high occurrence probability as 0.9. As specified in Equation 2, λ_D is the user's target occurrence probability of dynamic hazards. As specified in Equation 6, λ_F denotes the target occurrence probability for fall hazards; λ_C denotes that for caught-in/between hazards; and λ_E denotes that for electrical hazards. The following scenarios can be synthesized with different settings:

- *A Few Hazards*: A route with a few hazards: $\lambda_F = \lambda_C = \lambda_E = \lambda_D = 0.1$.
- *More Fall Hazards*: A route with more fall hazards: $\lambda_F = 0.9$, $\lambda_C = \lambda_E = \lambda_D = 0.1$.
- *More Caught-in/between Hazards*: A route with more caught-in/between hazards: $\lambda_C = 0.9$, $\lambda_F = \lambda_E = \lambda_D = 0.1$.
- *More Electrical Hazards*: A route with more electrical hazards: $\lambda_E = 0.9$, $\lambda_F = \lambda_C = \lambda_D = 0.1$.
- *More Dynamic Hazards*: A route with more dynamic (struck-by) hazards: $\lambda_D = 0.9$, $\lambda_F = \lambda_C = \lambda_E = 0.1$.
- *All Types of Hazard*: A route with a larger number of all types of hazards: $\lambda_F = \lambda_C = \lambda_E = \lambda_D = 0.9$.

Figure 8 shows the synthesis results with the corresponding type(s) of hazards emphasized. Note that in our user study experiments, for those users from the personalized VR training group, the target occurrence probabilities were computed according to how many mistakes the users had made for identifying each type of hazards in the pre-evaluation phase. Section 5 contains more details.

5 User Study Experiments

5.1 Implementation

We implemented our optimization-based approach for synthesizing VR training scenarios using C# and and the Unity game engine. The optimization was performed on a PC with 64 GB RAM and a 3.60Hz Intel(R) Core i7-9700K CPU processor. The synthesized VR training scenarios were deployed on an Oculus Quest 2 virtual reality headset which was used for user study experiments.

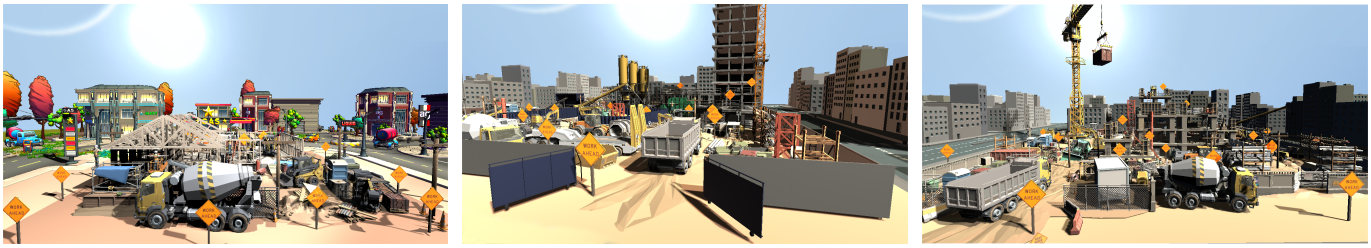

(a) Construction site 1 (a town house). (b) Construction site 2 (a shopping center). (c) Construction site 3 (a campus).

Fig. 9. Three virtual construction sites used for our user study. (a) Construction site 1 is used for pre-training. (b) Construction site 2 is used for VR training. (c) Construction site 3 is used for pre- and post-evaluation. By using different construction sites for training and evaluations, we avoid biases in the user study that users might repeat similar tasks in VR training that also appeared in evaluations if both scenarios were synthesized on the same construction site.

We conducted user study experiments to measure the effectiveness of the construction safety virtual training scenarios synthesized with our approach. Each user study consists of four sessions: (1) pre-training, (2) pre-evaluation, (3) training, and (4) post-evaluation. As shown in Figure 9, we designed three different construction sites applied to different sessions. The pre-training was performed on construction site 1. The VR training scenarios were synthesized on construction site 2. The pre-evaluation and the post-evaluation share the same training scenario synthesized on the construction site 3.

Participants. We recruited 45 participants among whom most were college students aged between 22 and 35 with an average age of 28.3. The ratio of male to female participants is 1.12. They were randomly recruited from different majors such as electrical engineering, computer science, data science, arts, etc. All of them had not received any construction safety training before. To compare the effectiveness of our synthesized personalized VR training with other types of training, the participants were randomly and evenly separated into three groups: one was the control group using slides training; one was the free exploration VR training group; and the remaining one was the personalized guidance VR training group.

5.2 Pre-Training

To mitigate the negative bias of user study results among the users who were not familiar with VR controllers, we prepared a pre-training session, which was a short warm-up training session, to get users familiar with how to use VR controllers correctly. During this session, the users from all groups were put into the first construction site with no performance evaluations recorded. The goal of pre-training was to let a user practice two basic operations: navigation control and answer selection. As shown in Figure 11, (a) navigation control operations were based on clicking a speed button on the left-hand controller. The operations included (1) start moving (one click), (2) stop moving (another click), and (3) speeding-up (holding the button down while moving).

When the user entered any hazardous region, the user would be asked to select the identified hazard type by clicking on a button showing the right hazard type choice (see Figure 11(b)) using the front trigger on the right-hand controller. The system would then record the user's choice. As the user indicated familiarity with the navigation control and answer selection, the user stopped the pre-training session. The user was then ready for the next training session.

5.3 Pre-Evaluation

The pre-evaluation is synthesized on the third construction site and optimized with the parameter settings: *All Types of Hazard* as specified in Section 4.2. In this session, users from all three groups are put into the same training scenario to evaluate their background knowledge of construction safety. Users who have no background in construction safety are encouraged to intuitively select the answers. As the accuracy of identifying different types of potential hazards is crucial for evaluating safety training effectiveness, we track the user's answers during the evaluation and compare their answers with the correct answers, the numbers of the mistakes that users have made for each type of hazards are counted. Please refer to the supplementary material for detailed evaluation tasks.

Fig. 10. Navigation approach of the free exploration VR training. Left controller's lightsaber is used to teleport to any location in the scene. The speed button on the left controller and the selection button on the right controller worked like those in the pre-training program as shown in Figure 11. In the example shown, the user was about to navigate to the anchor point highlighted as a blue shining pillar.

5.4 Training

There were three training conditions, which were experienced by the three groups of participants, respectively.

Slides Training. Under this training condition, the 15 participants from the control group were not trained using the synthesized training scenarios in the virtual scene. Instead, they were taught about fundamental construction safety knowledge through a short lecture presentation using slides. On the slides, there were real-world pictures showing examples of different types of hazards. During the presentation, a lecturer carefully went through each slide and explained each type of hazard. At the same time, the participants were encouraged to ask questions to make every key point clear. By the end of the training, the lecturer gave a Q&A session to make sure the participants fully understand the content covered in the lecture and were ready for the post-evaluation. Please refer to the supplementary material for details about the content of the lecture slides.

Free Exploration VR Training. Different from the control group without VR training, the 15 participants from the free exploration VR (FE-VR) group were trained with VR training scenarios synthesized on construction site 2 and optimized with the *All Types of Hazard* parameter settings as specified in Section 4.2. However, in this case, users did not navigate the construction site through the routes synthesized with our approach. Rather, they had the freedom to navigate arbitrarily in the scene by themselves. As shown in Figure 10, users can use the lightsaber shot from their left controller to teleport to any position in the scene. This navigation approach mimic the conventional and free exploration VR training programs commonly used [40, 50]. As guidance from an expert leads to a greater learning gain when compared to users' playing alone [3], we incorporate the instructor during the free exploration VR and personalized guidance VR training as well. During the free exploration VR training, the instructor would ask the users to slow down and inspect if there was any hazard around them. The instructor would explain why there were such types of hazards by

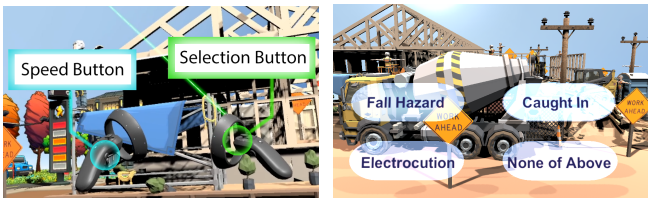

(a) Controllers. (b) Answer selection.

Fig. 11. Two operations on the controllers: (a) the left controller's button is used to control the navigation speed while the right controller's button is used to select the correct answers. (b) Four answer buttons popped up after the user entered a hazardous region. After a click of right front trigger, selected answer will be submitted.

pointing out the hazardous objects in VR. Sometimes if there was no obvious hazard around, the instructor still asked users whether there were any hazards. If the answer was yes, the instructor would correct the users' misunderstanding by explaining why there was no potential hazard. The maximum training time for the free exploration VR group was 15 minutes, which was 50% longer than the average training time for the personalized VR group which took about 10 minutes.

Personalized Guidance VR Training. Different from the free exploration VR (FE-VR) training group, the 15 participants of the personalized guidance VR (PG-VR) training group were trained with training scenarios synthesized based on their performance in the pre-evaluation. Given different parameters settings defined in Section 4.2, the users would be trained by different personalized training scenarios synthesized according to how many mistakes they have made for each type of hazards during the pre-evaluation. More specifically, the parameter settings, namely, λ_F, λ_C, and λ_E, were calculated by the users' mistake rates for identifying each type of hazards respectively. For example, for detecting fall hazards, if the user got 3 out of 4 incorrect answers in pre-evaluation, then $\lambda_F = 3/4 = 0.75$. Our optimization approach would then run according to the parameter settings computed this way to synthesize the personalized guidance VR training scenarios. Note that both free exploration and personalized guidance VR training scenarios were synthesized on construction site 2. By doing so, we avoided the similarity of the training scenarios with the scenario used in pre- and post-evaluation, which is synthesized on construction site 3.

5.5 Post-Evaluation

To investigate whether the users' accuracy in identifying different types of hazards had improved after going through different training conditions, the same tasks in the pre-evaluation were assigned to the users again in a post-evaluation session. In this session, the instructor gave no hints or suggestions to the users. Similar to the pre-evaluation, the correctness of the users' answers was evaluated. After the users completed the assigned post-evaluation tasks, the users were prompted to complete a questionnaire. The questionnaire included different questions for feedback on the virtual evaluation tasks, virtual training tasks (if applicable), and the effectiveness of our training programs.

6 Results and Discussion

Figure 12 shows the error bar plots of the number of mistakes users made on each type of hazard during the pre- and post-evaluation. Darker colors represent the average number of mistakes made in the pre-evaluation, while the lighter colors represent those in the post-evaluation. Different types of hazards are represented with different colors: blue denotes the fall hazards, orange denotes the caught-in/between hazards, and green denotes the electrical hazards. We analyze the results of users' accuracy in hazard inspection from the pre- and post-evaluations. Please refer to Figure 5 in supplementary material for the number of mistakes made by each participant.

We compare the difference between users' improvements from slides training group, free exploration VR training group, and personalized guidance VR training group. Note that during our synthesized training, users were prompted to avoid the dynamic hazards (i.e. struck-by

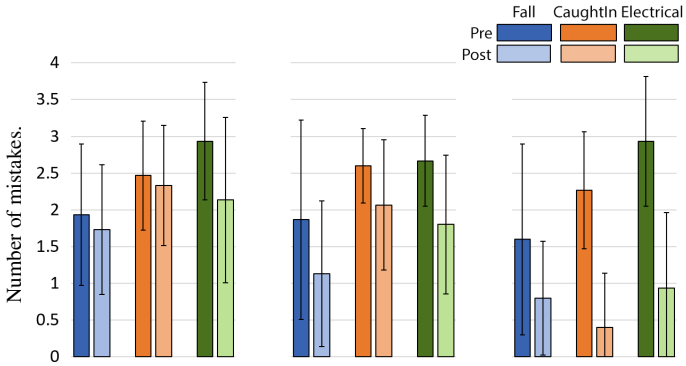

(a) Slides group. (b) FE-VR group. (c) PG-VR group.

Fig. 12. Inspection errors. These error bar plots show the average number of mistakes users made on inspecting each type of hazard during the pre- and post-evaluation. Darker colors represent the number of mistakes made in pre-evaluation while lighter colors represent those in post-evaluation. Blue, orange, and green colors denote the errors made on inspecting fall, caught-in/between, and electrical hazards, respectively.

hazards). If the user is not able to avoid them on time, there will be warnings popped up to show that they were struck by the dynamic hazards. In the preliminary test of our VR training program, we realize that the dynamic hazards designed in this way were very obvious to be identified due to their movements and there was generally no difference in the user performance in identifying them before and after training. So, we did not count the number of errors related to dynamic hazards.

Statistical Analysis. Given the experimental results, we evaluate users' improvements according to the reduction in the number of mistakes they have made in the pre-evaluation and the post-evaluation. As shown in Figure 13, the improvements of users from different groups are represented with different colors, among which the slides training group (Slides), free exploration VR training group (FE-VR) and personalized guidance VR training group (PG-VR) are colored as blue, orange and green, respectively. According to the descriptive statistics, the total average improvement for the slides group, free exploration VR group, and personalized guidance VR group are 1.13, 2.13, and 4.66, respectively. In general, users from all three groups have improved their accuracy in identifying different types of hazards. On average, the VR training groups improve more than the slides group, and the personalized guidance VR training group improves more than the free exploration VR training group. According to the descriptive statistics for each type of hazard, for those users from the slides group, the average improvement in inspecting the fall hazards, the caught-in/between hazards, and the electrical hazards are 0.2, 0.13, and 0.8, respectively. Similarly, for FE-VR group, the average improvements are 0.73, 0.53, and 0.86, respectively. For PG-VR group, they are 0.8, 1.87, and 2, respectively.

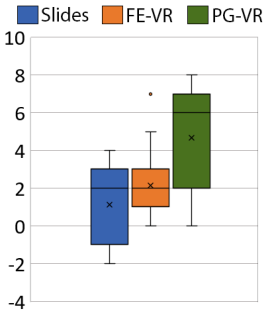

Fig. 13. Users' improvement.

Furthermore, we analyze whether there is any statistically significant difference between the improvement made by the users from the three groups. We applied two factors ANOVA tests (with Scheffe test as a post hoc test) [9] for users' improvement on each type of hazard. Using $\alpha = 0.05$ (95% confidence interval), we obtain the ANOVA test results showing that among the three different groups, $p = 0.00026 < 0.05$. Therefore, with a 95% confidence level, we reject the null hypothesis that there is no statistically significant difference between the improvements made by the users from different groups. Furthermore, according to a post hoc test, when comparing the FE-VR group with the slides group, we obtain $p = 0.47 > 0.05$; when comparing the PG-VR group with the FE-VR group, we obtain $p = 0.012 < 0.05$; when comparing the PG-VR group with the slides group, we obtain $p = 0.0004 < 0.05$. Therefore, with a 95% confidence level, we conclude that the users

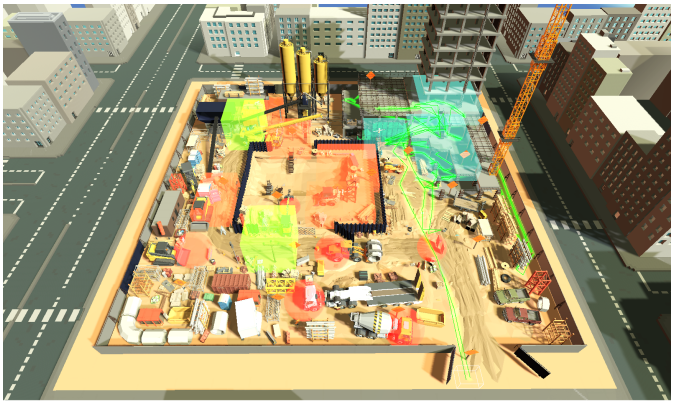

Fig. 14. A user navigation example. A user from the free exploration VR group was not able to explore the training scene efficiently. The green curve is the user's navigation path during the training. The user only passed through the regions with fall hazards (in blue), while he missed all regions with caught-in/between hazards (in yellow) and electrical hazards (in green). This results in poor improvement in his skills as reflected by his performance in the post-evaluation, where he shows improvement in his fall hazard inspection skill but has no improvement in detecting all other types of hazards.

from the PG-VR group improve significantly more than the FE-VR group and slides group.

User Navigation. Statistical analysis results suggest that personalized guidance VR training is more effective than free exploration VR training in improving the users' hazard identification skill. According to the observations, we believe that using the synthesized training route in the personalized guidance VR training scenarios may have led to the improvement, compared to having the users freely navigate in a free exploration VR training. Figure 14 shows a user navigation example. The green curve is the user's navigation path during the free exploration VR training. This users' number of mistakes in the pre-evaluation and post-evaluation are plotted as the last pair of columns in Figure 5 (b) in the supplementary material. More specifically, in pre-evaluation, the number of mistakes this user made for fall, caught-in/between, and electrical hazards are 4 ,2 and 3 respectively. In post-evaluation, they are 0, 3, and 3, respectively. As we can see, this user had corrected all of the mistakes in identifying fall hazards while he had no improvement at all in detecting other types of hazards. This is likely because this user had only navigated to the areas of the scene where there were fall hazards only (top-right under the blue shade), therefore he got no chance to be trained on detecting other types of hazards. Rather, as shown in Figure 8, personalized guidance VR training would address all of the users' weak points by guiding them towards the hazards they were not quite familiar with. This setting may explain why some of the users from the free exploration VR training group improved much less than those from the personalized guidance VR training group. However, we believe that if the users from free exploration VR training group were given plenty of time, they could have improved as much as the users from personalized guidance VR training group. Note that, as mentioned before, the users from the free exploration VR training group has been given a 50% longer time than the personalized guidance VR training group. On the other hand, compared to slides group, the training time is generally the same as the PG-VR group. Which means, users in PG-VR group are given sufficient amount of time in exploring the scene. This suggests that the personalized guidance VR training is more efficient than the free exploration VR training. We also note that longer VR training time more likely result in dizziness and vertigo, so, improving training efficiency of VR training is important.

Common Mistakes. We discuss some common mistakes made by the users in the in both pre and post evaluations. As shown in Figure 15, such common mistakes include (a) mistakening struck-by hazards as fall hazards; (b) mistakening caught-in/between hazards as fall hazards; (c) missing electrical hazards; and (d) missing caught-in/between hazards. Users sometimes make those common mistakes again even after the training process. However, those users from the slides group and free exploration VR group tend to make those mistakes again more often than the personalized guidance VR group. Reasons for those mistakes are concluded as follows:

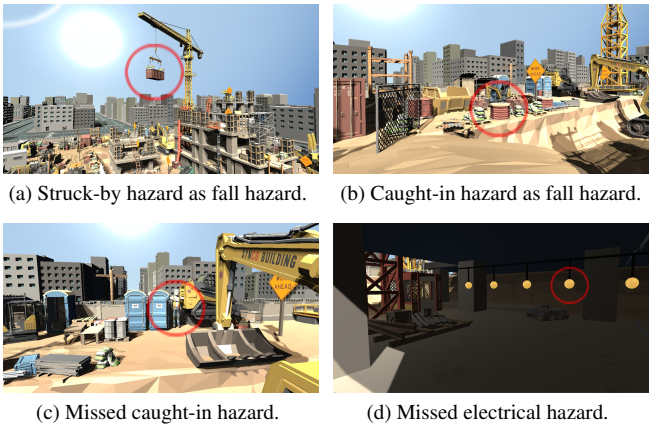

(a) Struck-by hazard as fall hazard. (b) Caught-in hazard as fall hazard.

(c) Missed caught-in hazard. (d) Missed electrical hazard.

Fig. 15. Examples of common mistakes. (a) struck-by hazard is mistaken as fall hazard; (b) caught-in/between hazard is mistaken as fall hazard; (c) missed caught-in/between hazard; and (d) missed electrical hazard.

- Struck-by hazards as fall hazards. Users misinterpreted the falling objects as fall hazards. In fact, falling objects which could strike people belong to struck-by hazards.
- Caught-in/between hazards as fall hazards. Users misinterpreted that objects near a cave caused fall hazards. In fact, heavy objects near the rim of a cave could cause the cave to collapse and bury the people working inside the cave. This is called a cave-in hazard, belongs to caught-in/between hazard.
- Missed caught-in/between hazards. Some users missed pointing out the risk of being caught-in between two objects and potentially being crushed from two sides.
- Missed electrical hazards. Some users failed to identify the risk caused by electrical components such as temporary lights suspended by electric cords. Exposing to damaged wires with high voltage could result in electric shocks and death.

User Feedback. In order to learn from user's feeling about our designed virtual environment for evaluations and trainings, we asked users to fill out questionnaires after the study and collected their general feedbacks. The results are shown in Figure 16. Most of the users agree with the following: our VR construction safety training and evaluation programs are realistic and comfortable; the animation of VR construction simulations looks natural; the control of VR navigation feels natural; the training tasks in VR or slides are enjoyable. Most of the users believe that through the training (either by VR or by slides), their construction safety knowledge and skills have improved. On the other hand, most of the users think that the post-evaluation is easier than the pre-evaluation, even though they were based on the same construction scenario. This is reasonable since users had learned about the definitions and risks of different types of hazards through the training sessions (either by slides or VR) such that when they faced the same situations in the post-evaluation, they could apply their safety knowledge to assess the situations more confidently.

7 Summary

We have devised an optimization-based approach to synthesize personalized training scenarios for construction safety training in virtual reality. We developed several virtual scenes for different construction sites, generated the navigation meshes for the scenes, and incorporated different types of common hazards such as struck-by, fall, caught-in/between, and electrical into the scenes. By specifying some points

of interest as vertices, our approach generates a navigation path between every two vertices, resulting in a k-regular navigation graph with k-shortest distance paths. As shown in Figure 8, by optimizing the navigation route along with the sequence of hazards simultaneously and automatically, our approach can synthesize personalized training scenarios with emphasis on different types of hazards to efficiently improve a trainee's specific skills.

In order to measure the difference between our proposed personalized VR training method and the other two training methods, including slides training and free exploration VR training, we separated the users into three groups. We applied ANOVA tests to analyze users' improvement in hazard inspection with different training methods. The results show that users from the personalized guidance VR group improved more significantly than users from the other groups. We collected the users' feedback on their training experiences via questionnaires. We find that most users agree that our VR construction safety training and evaluation programs are realistic, immersive, and enjoyable.

Limitations and Future Work. The main limitation of our work is that the FE-VR condition confounds free exploration with the intended non-personalized condition, in comparison to the PG-VR condition, which employs guided exploration and the intended personalized condition. Therefore, future work should consider the fourth condition with guided exploration but not personalized to better understand whether the current significant differences between the FE-VR and PG-VR conditions are primarily due to personalized features or guided exploration.

Besides, despite most users like our VR training and evaluation programs, for example, according to users' feedback, some users liked the question settings and the construction sites where hazardous objects are realistically placed, some users liked the feeling of being guided by the auto-navigation. However, some users felt a little dizzy when they tried speeding up. Some users thought that the VR training would not be comfortable for older people. Please refer to the supplementary material for more details of the users' feedback.

We are also interested in the following future explorations that may enhance users' construction safety training experiences in virtual reality. For example, we can provide more hazard inspection tasks or increases the number of surrounding hazardous objects to avoid long tedious navigation which may cause dizziness. We can also increase the scale of construction sites and incorporate more diverse types of hazards to make the virtual training more comprehensive. The VR training program can also be extended to include VR manipulations such as training users to remove the hazards properly and safely rather than merely identifying potential hazards. We can also add narrations to the VR training to teach users about the concepts and definitions of different types of hazards. Overall, future work could focus on continuously improving the immersiveness and realism of virtual training experiences, leverging advances in VR tracking, locomotion, haptic feedback, and audio devices, etc.

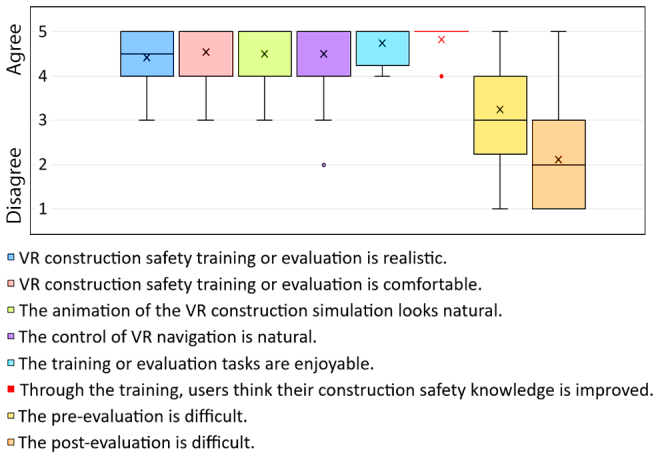

Fig. 16. Users' feedback about our developed construction safety VR training and evaluation programs.

ACKNOWLEDGMENTS

This research is supported by the National Science Foundation under award numbers 1942531 and 2128867.

REFERENCES

[1] K. Aati, D. Chang, P. Edara, and C. Sun. Immersive work zone inspection training using virtual reality. *Transportation Research Record*, p. 0361198120953146, 2020.

[2] A. Akintoye. Analysis of factors influencing project cost estimating practice. *Construction Management & Economics*, 18(1):77–89, 2000.

[3] P. Apostolellis and D. A. Bowman. Small group learning with games in museums: effects of interactivity as mediated by cultural differences. In *Proceedings of the 14th International Conference on Interaction Design and Children*, pp. 160–169, 2015.

[4] P. Apostolellis and D. A. Bowman. Audience involvement and agency in digital games: effects on learning, game experience, and social presence. In *Proceedings of the The 15th International Conference on Interaction Design and Children*, pp. 299–310, 2016.

[5] V. Benjaoran and S. Bhokha. An integrated safety management with construction management using 4d cad model. *Safety Science*, 48(3):395–403, 2010.

[6] G. Benvegnù, P. Pluchino, and L. Garnberini. Virtual morality: Using virtual reality to study moral behavior in extreme accident situations. In *2021 IEEE Virtual Reality and 3D User Interfaces (VR)*, pp. 316–325. IEEE, 2021.

[7] S. Bhoir and B. Esmaeili. State-of-the-art review of virtual reality environment applications in construction safety. In *AEI 2015*, pp. 457–468. 2015.

[8] A. E. Brouwer and W. H. Haemers. Distance-regular graphs. In *Spectra of Graphs*, pp. 177–185. Springer, 2012.

[9] G. Casella. *Statistical design*. Springer Science & Business Media, 2008.

[10] M. Chester and C. Hendrickson. Cost impacts, scheduling impacts, and the claims process during construction. *Journal of construction engineering and management*, 131(1):102–107, 2005.

[11] S. Chib and E. Greenberg. Understanding the metropolis-hastings algorithm. *The american statistician*, 49(4):327–335, 1995.

[12] R. M. Clifford, S. Jung, S. Hoermann, M. Billinghurst, and R. W. Lindeman. Creating a stressful decision making environment for aerial firefighter training in virtual reality. In *2019 IEEE Conference on Virtual Reality and 3D User Interfaces (VR)*, pp. 181–189. IEEE, 2019.

[13] C. Di Loreto, J.-R. Chardonnet, J. Ryard, and A. Rousseau. Woah: A virtual reality work-at-height simulator. In *2018 IEEE Conference on Virtual Reality and 3D User Interfaces (VR)*, pp. 281–288. IEEE, 2018.

[14] R. Eiris, M. Gheisari, and B. Esmaeili. Desktop-based safety training using 360-degree panorama and static virtual reality techniques: A comparative experimental study. *Automation in Construction*, 109:102969, 2020.

[15] H. Furuya, K. Kim, G. Bruder, P. J. Wisniewski, and G. F. Welch. Autonomous vehicle visual embodiment for pedestrian interactions in crossing scenarios: Virtual drivers in avs for pedestrian crossing. In *Extended Abstracts of the 2021 CHI Conference on Human Factors in Computing Systems*, pp. 1–7, 2021.

[16] M. Gheisari and B. Esmaeili. Pars: Using augmented panoramas of reality for construction safety training. *Silver Spring, MD: CPWR-The Center for Construction Research and Training*, 2019.

[17] P. J. Green. Reversible jump markov chain monte carlo computation and bayesian model determination. *Biometrika*, 82(4):711–732, 1995.

[18] A. S. Hanna, C. S. Taylor, and K. T. Sullivan. Impact of extended overtime on construction labor productivity. *Journal of construction engineering and management*, 131(6):734–739, 2005.

[19] S. Hasanzadeh, B. Esmaeili, and M. D. Dodd. Measuring the impacts of safety knowledge on construction workers' attentional allocation and hazard detection using remote eye-tracking technology. *Journal of management in engineering*, 33(5):04017024, 2017.

[20] K. Hines, W. Lages, N. Somasundaram, and T. Martin. Protecting workers with smart e-vest. In *Adjunct Proceedings of the 2015 ACM International Joint Conference on Pervasive and Ubiquitous Computing and Proceedings of the 2015 ACM International Symposium on Wearable Computers*, pp. 101–104, 2015.

[21] H. Huang, N.-C. Lin, L. Barrett, D. Springer, H.-C. Wang, M. Pomplun,

and L.-F. Yu. Automatic optimization of wayfinding design. *IEEE transactions on visualization and computer graphics*, 24(9):2516–2530, 2017.

[22] B.-G. Hwang, S. R. Thomas, C. T. Haas, and C. H. Caldas. Measuring the impact of rework on construction cost performance. *Journal of construction engineering and management*, 135(3):187–198, 2009.

[23] H. Karimi, T. R. Taylor, and P. M. Goodrum. Analysis of the impact of craft labour availability on north american construction project productivity and schedule performance. *Construction Management and Economics*, 35(6):368–380, 2017.

[24] S. Kirkpatrick, C. D. Gelatt, and M. P. Vecchi. Optimization by simulated annealing. *science*, 220(4598):671–680, 1983.

[25] Y. Lang, W. Liang, F. Xu, Y. Zhao, and L.-F. Yu. Synthesizing personalized training programs for improving driving habits via virtual reality. In *IEEE Virtual Reality*, 2018.

[26] Q. T. Le, A. Pedro, and C. S. Park. A social virtual reality based construction safety education system for experiential learning. *Journal of Intelligent & Robotic Systems*, 79(3-4):487–506, 2015.

[27] H. Li, G. Chan, and M. Skitmore. Multiuser virtual safety training system for tower crane dismantlement. *Journal of Computing in Civil Engineering*, 26(5):638–647, 2012.

[28] H. Li, M. Lu, S.-C. Hsu, M. Gray, and T. Huang. Proactive behavior-based safety management for construction safety improvement. *Safety science*, 75:107–117, 2015.

[29] W. Li, J. Talavera, A. G. Samayoa, J.-M. Lien, and L.-F. Yu. Automatic synthesis of virtual wheelchair training scenarios. In *IEEE Virtual Reality*, 2020.

[30] W. Li, B. Xie, Y. Zhang, W. Meiss, H. Huang, and L.-F. Yu. Exertion-aware path generation. *ACM Transactions on Graphics (TOG)*, 39(4):115–1, 2020.

[31] W. Liang, J. Liu, Y. Lang, B. Ning, and L.-F. Yu. Functional workspace optimization via learning personal preferences from virtual experiences. *IEEE transactions on visualization and computer graphics*, 25(5):1836–1845, 2019.

[32] F. Lin, L. Ye, V. G. Duffy, and C.-J. Su. Developing virtual environments for industrial training. *Information Sciences*, 140(1-2):153–170, 2002.

[33] F. Mantovani and G. Castelnuovo. The sense of presence in virtual training: enhancing skills acquisition and transfer of knowledge through learning experience in virtual environments. 2003.

[34] B. McTague and G. Jergeas. *Productivity improvements on Alberta major construction projects: Phase I-Back to basics*. Alberta economic development, 2002.

[35] H. F. Moore, R. Eiris, M. Gheisari, and B. Esmaeili. Hazard identification training using 360-degree panorama vs. virtual reality techniques: A pilot study. In *Computing in Civil Engineering 2019: Visualization, Information Modeling, and Simulation*, pp. 55–62. American Society of Civil Engineers Reston, VA, 2019.

[36] F. Palmas, R. Reinelt, J. E. Cichor, D. A. Plecher, and G. Klinker. Virtual reality public speaking training: Experimental evaluation of direct feedback technology acceptance. In *2021 IEEE Virtual Reality and 3D User Interfaces (VR)*, pp. 463–472. IEEE, 2021.

[37] R. E. Pereira, M. Gheisari, and B. Esmaeili. Using panoramic augmented reality to develop a virtual safety training environment. *Constr. Res. Congr*, pp. 29–39, 2018.

[38] G. Quenell. Spectral diameter estimates for k-regular graphs. *Advances in mathematics*, 106(1):122–148, 1994.

[39] F. D. Rose, E. A. Attree, B. M. Brooks, D. M. Parslow, and P. R. Penn. Training in virtual environments: transfer to real world tasks and equivalence to real task training. *Ergonomics*, 43(4):494–511, 2000.

[40] R. Sacks, A. Perlman, and R. Barak. Construction safety training using immersive virtual reality. *Construction Management and Economics*, 31(9):1005–1017, 2013.

[41] R. D. B. X. S. D. Samantha Brown, William Harris. Fatal injury trends in the construction industry. *CPWR The Center for Construction Research and Training (CPWR 2021)*, `https://www.cpwr.com/wp-content/uploads/DataBulletin-February-2021.pdf`.

[42] C. Sinnott, J. Liu, C. Matera, S. Halow, A. Jones, M. Moroz, J. Mulligan, M. Crognale, E. Folmer, and P. MacNeilage. Underwater virtual reality system for neutral buoyancy training: Development and evaluation. In *25th ACM Symposium on Virtual Reality Software and Technology*, pp. 1–9, 2019.

[43] P. J. Van Laarhoven and E. H. Aarts. Simulated annealing. In *Simulated annealing: Theory and applications*, pp. 7–15. Springer, 1987.

[44] Y. Wang, P. M. Goodrum, C. T. Haas, and R. W. Glover. Craft training issues in american industrial and commercial construction. *Journal of construction engineering and management*, 134(10):795–803, 2008.

[45] G. Westerfield, A. Mitrovic, and M. Billinghurst. Intelligent augmented reality training for motherboard assembly. *International Journal of Artificial Intelligence in Education*, 25(1):157–172, 2015.

[46] B. Xie, Y. Zhang, H. Huang, E. Ogawa, T. You, and L.-F. Yu. Exercise intensity-driven level design. *IEEE transactions on visualization and computer graphics*, 24(4):1661–1670, 2018.

[47] H. Xie, E. Tudoreanu, and W. Shi. Development of a virtual reality safety-training system for construction workers. *Digital library of construction informatics and information technology in civil engineering and construction*, 2006.

[48] L. Zhang, D. A. Bowman, and C. N. Jones. Exploring effects of interactivity on learning with interactive storytelling in immersive virtual reality. In *2019 11th International Conference on Virtual Worlds and Games for Serious Applications (VS-Games)*, pp. 1–8. IEEE, 2019.

[49] Y. Zhang, B. Xie, H. Huang, E. Ogawa, T. You, and L.-F. Yu. Pose-guided level design. In *Proceedings of the 2019 CHI Conference on Human Factors in Computing Systems*, pp. 1–12, 2019.

[50] D. Zhao and J. Lucas. Virtual reality simulation for construction safety promotion. *International journal of injury control and safety promotion*, 22(1):57–67, 2015.